PROCEEDINGS, Thirty-Seventh Workshop on Geothermal Reservoir Engineering
Stanford University, Stanford, California, January 30 - February 1, 2012
SGP-TR-194

SYSTEM AND METHODOLOGY FOR RAPID EVALUATION OF GEOTHERMAL ROCK-FLUID INTERACTIONS ASSOCIATED WITH CO_2-EGS

Miroslav Petro[1], Li Song[1], Alan Bell[1], Alexander Tuganov[1], Keshav Parajuly[1], Patrick Dobson[2], Tianfu Xu[2], Karsten Pruess[2]

[1]Palo Alto Research Center (PARC)
3333 Coyote Hill Road, Palo Alto, CA 94304
e-mail: mpetro@parc.com

[2]Lawrence Berkeley National Laboratory (LBNL)
One Cyclotron Road, Berkeley CA 94720

ABSTRACT

Numerical simulations of Enhanced Geothermal Systems with CO_2 as the heat transmission fluid (CO_2-EGS) are optimistic. However, there is always water present underground, and transition from aqueous to dry supercritical CO_2 environments is accompanied by a series of complex rock-fluid interactions, which significantly affect both overall capacity and lifetime of a CO_2-EGS reservoir. Therefore, focused experimentation characterizing CO_2-H_2O-mineral reactions and interactions is necessary to understand this process and validate the expected outcomes. The results of the batch and flow-through reactor experiments will be used to determine mineral equilibrium solubility values and kinetic reaction rates over a range of pressure, temperature, and fluid composition conditions. These data can then be used to constrain coupled process simulations of CO_2-EGS reservoir behavior, thus yielding more realistic predictions.

For such a purpose, PARC has developed an integrated multichannel reactor system, fed by a mixture of gases, liquids and supercritical fluids, operating in a wide range of high-pressure and high-temperature conditions, and coupled to an on-line diagnostics system for real-time detailed ion analysis.

The data are generated in collaboration with LBNL, utilizing their expertise in geothermal reservoir modeling with an extensive history of CO_2 applications. Jointly, we can mimic a variety of geothermal-like situations by rapidly screening behavior of relevant minerals for their solubilities across the water-CO_2 interface, or monitor an accelerated dissolution process of diverse rock formations in an underground setting.

The applications of interest include mapping out transition of a reservoir from water to dry supercritical CO_2, understanding the role of naturally dissolved gasses and minerals on development of underground water pathways, predicting the effect of injected water compositions on native rock solubility, assessing risks and benefits associated with precipitation-redissolution processes during reservoir stimulation, and many others.

INTRODUCTION

As revealed in the MIT report on the U.S. geothermal potential (Tester et al., 2006), there is an abundance of heat but lack of fluids underground. This has revitalized the original idea of using supercritical CO_2 in a hot dry rock reservoir (Brown 2000), and triggered an avalanche of interest in related issues.

Advanced modeling software such as TOUGHREACT (Xu et al., 2006) was found useful to simulate a CO_2-based working fluid for an EGS reservoir, taking into account fluid dynamics and heat transfer issues (Pruess 2006, 2008), performing chemically reactive transport modeling including some fluid-rock interactions (Steefel et al., 2005, Wan et al., 2011). A similar coupled process approach has been utilized to evaluate CO_2-mineral reactions associated with carbon sequestration (e.g., Andre et al., 2010).

Along with reporting on advantages of using CO_2-EGS, there are an increasing number of reports on significant challenges associated with introduction of CO_2 into reservoirs containing at least some traces of water, using laboratory experiments or reservoir data. For example, laboratory data showed that CO_2 injection leads to an increase in brine density (Garcia 2001), thus triggering compositionally driven instability and convective fingering (Kneafsey and Pruess, 2010). Much less is known about behavior of dry CO_2. For example, even traces of water in otherwise dry CO_2 make the fluid chemically active and prone to various surprises when interacting with

minerals (McGrail et al., 2009, Regnault et al., 2005), including collapse of crystalline or amorphous structures due to dehydration of mineral-bound water, thus possibly increasing permeability and promoting the reservoir growth (Pruess and Azaroual, 2006). Despite discrepancies between the results of experiments and simulations, there is a close agreement on overall trends in mineral alteration, fluid chemistry, and permeability evolution (Morrow et al., 2001, Palguta et al., 2011, Xu et al., 2004).

While some researchers are addressing generic issues, others are trying to turn the knowledge into heat harvesting scenarios applicable to existing reservoirs. As examples of recent efforts, there is a consideration of CO_2 injection into a Gulf of Mexico geopressured aquifer with a geomodel of subsequent wellbore cooling (Plaksina et al., 2011), or plan for co-injection of CO_2 into a small geothermal reservoir to store CO_2 simultaneously with hot-water extraction (Salimi et al., 2011).

Previous experimentation and modeling shows that not only during the water-to-CO_2 transition, but even in fully developed CO_2-EGS reservoirs, there would still be three distinct zones present – a core region dominated by a supercritical CO_2 fluid phase, a surrounding intermediate zone, and peripheral region containing an aqueous phase with dissolved CO_2 (Liu et al., 2003, Fouillac et al., 2004, Ueda et al., 2005, Pruess 2008, Wan et al., 2011). As different fluid zones will contain different rocks composed of diverse minerals, a whole series of mineral dissolution, precipitation, and re-dissolution reactions may evolve, altering the pathways of heat-mining fluid and contact area for rock-fluid heat exchange. More experimental data are necessary to better understand mineral behavior in all of these zones and, especially, at their interfaces, covering a variety of local pressure, temperature and other conditions.

We believe that advanced experimental systems combined with proven modeling approaches, as presented in this paper, will enable the geothermal industry to predict the flow of underground fluids and truly assess both risks and benefits of CO_2-EGS operation.

EXPERIMENTAL

The centerpiece of the PARC Geothermal system is a large oven, with the ability to heat up to 300 ^oC and a set of pumps that can push up to 30 MPa of fluid pressure into 50 mL reactors. Figure 1 shows the whole system as well as its individual components, with a suite of five high-pressure / high-temperature reactors inside the oven, connected to the feed and sampling components via complex electrical and fluidic pathways, with a control center outside of the oven. To extend the experimental temperature range, we have equipped reactors with additional heaters, which will allow us to perform certain experiments well above the oven temperature. While extreme conditions are possible, most of the routine operation is performed in the 120-180 ^oC and 8-14 MPa range, as some other components such as valves can survive only a relatively short exposure to extremes outside of their comfort zone.

Figure 1 – PARC Geothermal Interaction System. *Individual components include: Oven (1), Reactor cell assembly (2), Stirring assembly (3), Dip-tube CO_2 cylinder (4), CO_2 feed pump (5), Water-feed pump (6), Sample withdrawal pump (7), Sample analysis pump (8), Mineral concentration detector (9), System control & Data acquisition station (10), and Multi-channel reactor configuration (bottom).*

The mineral samples used in this study (calcite, dolomite, anorthite, microline, siderite, biotite, quartz and barite) were purchased from Ward's Natural Science, Rochester, NY. The rock/mineral samples are grounded in the attritor mill from Union Process, Akron, OH, and subsequently sieved into two particle size groups: 25-63 μm and 63-150 μm range. The powders are cleaned to remove any attached very fine particles by repeated sedimentation in DI water. The cleaned mineral samples are then air dried at 90 ^oC for more than 20 hours to remove physically adsorbed water. Optical microscopy is used to inspect the samples for imparities and particle size distributions. The whole sample preparation workflow is depicted in Figure 2.

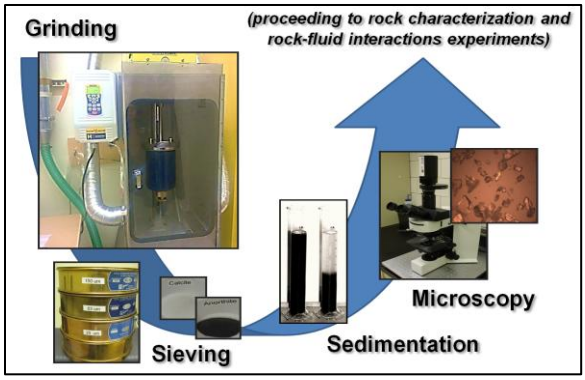

Figure 2 – Sample preparation workflow.

In the subsequent rock characterization process, an aliquot of each sample was sent to Burnham Petrographics for polished thin section preparation. The polished thin sections were then examined and photographed using a petrographic microscope. Selected grains were analyzed using a Cameca SX-51 electron microprobe equipped with 5 tunable wavelength dispersive spectrometers at the UC Berkeley microprobe facility. An aliquot of each mineral sample was also submitted to the XRD facility for crystallographic analysis at the UC Berkeley Earth and Planetary Sciences Department. Figure 3 shows a photomicrograph and XRD pattern for the 63-150 micron-sized anorthite sample.

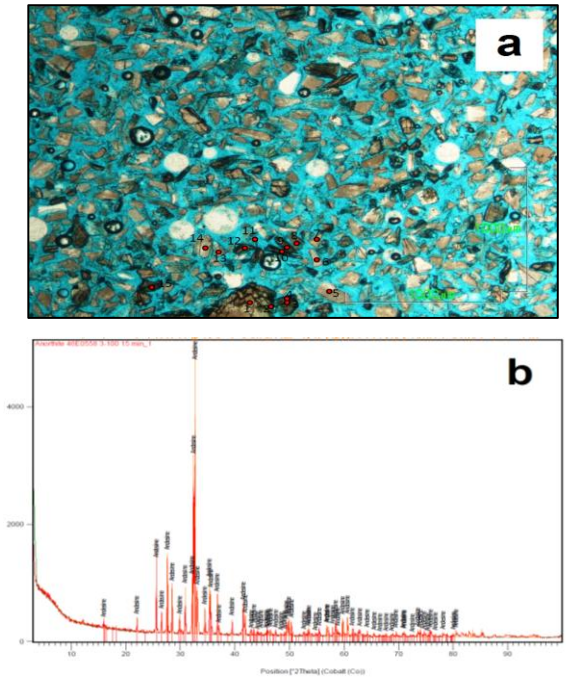

Figure 3 – Anorthite characterization results.
Photomicrograph using uncrossed nicols (a), with red dots indicating microprobe analysis points; and the XRD pattern for the same sample (b).

Electron microprobe analyses of both chunk and grain "anorthite" samples indicated that the plagioclase feldspar was not really in the form of anorthite (as classified by the vendor), but instead it appears to be labradorite in composition $An_{60}Ab_{40}$, containing small amounts of a Fe-Mg rich aluminosilicate alteration phase (most likely either chlorite or amphibole) replacing feldspar. The average normalized composition (wt. %) of the plagioclase grains is: 51.9% SiO_2, 30.5% Al_2O_3, 0.03% TiO_2, 0.30% FeO, 0.02% MnO, 0.04% MgO, 12.8% CaO, 4.3% Na_2O, 0.1% K_2O, and 0.01% BaO.

Most of the other mineral samples that have been analyzed to date, including calcite and dolomite, were close to stoichiometric in composition, but it is apparent that even the cleanest mineral separates are not absolutely pure, but often contain minor amounts of additional minerals as alteration phases or inclusions.

For the batch rock-fluid interaction experiments, after weighing in desired amounts of crushed and sieved rock samples into individual reactors, the water and supercritical CO_2 feeds are delivered to the reactor vessels using syringe pumps. Then, the rock particles are mixed with water and supercritical CO_2 into slurry, optionally stirred by a high-torque stirrer. Since dissolution may start immediately upon contact of rock sample with fluids, therefore, the system is brought up to the operating temperature and pressure conditions as quickly as possible. The interaction conditions are monitored by thermocouples and pressure transducers at several points, and optionally by a conductivity or pH sensor built inside a larger reactor that could be connected for a special study. Once the reaction conditions are reached, small aliquots of the reaction mixture (typically 200 μL) are sampled and analyzed through the synchronized action of the sampling pump, selection valve, sampling valve, sample analysis pump, ion separation column, and mineral concentration detector. While the small fluid sample travels to the on-line connected ion-exchange High-Performance Liquid Chromatography (HPLC) system for detailed ion analysis, it is filtered and diluted in a strong solvent environment to insure that the dissolved components stay in solution.

The ion analysis is based on separation of individual solutes according to the charge they carry, followed by evaporative light-scattering detection (ELSD),

producing a concentration trace with peaks that represent each individual mineral component. After a calibration, the HPLC-ELSD method can yield the total dissolved mass (integrated ELSD signal), as well as the concentrations of each individual ion (ELSD peak areas) at any given sampling time. The sampling and analysis step is repeated for each experiment on a regular interval ranging from tens of minutes to up to several hours. Either helium or CO2 is used to keep the reactor at constant pressure after each fluid sampling.

As expected from the prior mineral sample characterization explained above, a number of impurities have been detected along with the main dissolved mineral components, and some of them positively identified, quantified, and confirmed by unrelated techniques. These impurities complicate the analysis and make the use of an ion separation technique absolutely necessary. Figure 4 shows some typical HPLC-ELSD traces for several minerals in our study. Currently, only mono- and bi-valent cations are separated and quantified using this method.

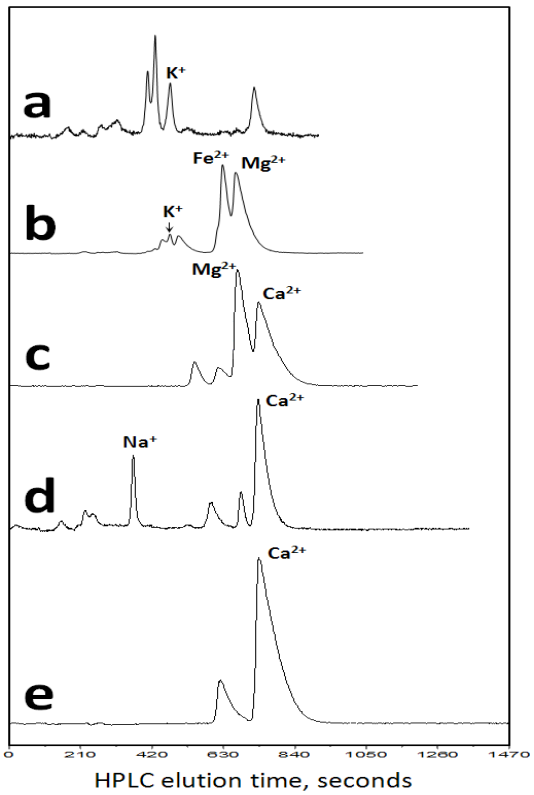

Figure 4 – Typical ion HPLC-ELSD traces.

Microline (a), biotite (b), dolomite (c), anorthite (d), and calcite (e).

RESULTS & DISCUSSION

Each experimental result is defined by a combination of input parameters, such as the rock sample descriptors, including mineral composition (if known), average particle size, reaction temperature, pressure and fluid composition. Control over the individual components of the whole system is provided by custom-made PARC software. The instrument control modules are combined with data-acquisition software that collects mineral concentration traces during the course of the experiment. Then, the experimental inputs, with actual pressure and temperature stamps at the sampling points, are linked to the mineral concentration traces and, after a calibration of our mineral ion detector, turned into the final solubility data at the specific interaction conditions. All of the inputs and corresponding outputs are collected into a simple worksheet table, which can be used to cross-correlate the equilibrium solubility values. These solubility data can be then compared with those used in the existing TOUGHREACT thermodynamic database and other published experimental results (e.g., Rosenbauer et al., 2005). The new data, which cover a wide range of P-T-X conditions for CO_2-rich fluids, are expected to be included in this database to create more realistic model of a CO_2-EGS reservoir.

When selecting the minerals for our study, we took into account that many geothermal systems are associated with igneous rocks, ranging from basalt/diabase to rhyolite/granite (extrusive vs. intrusive equivalent). The first group has typical mineralogies of plagioclase feldspar, clinopyroxene, olivine, and orthopyroxene, the second is composed of quartz, potassium feldspar, plagioclase feldspar, hornblende, biotite, +/- muscovite. These rocks often have undergone hydrothermal alteration, which results in the generation of alteration (secondary) mineral phases. Therefore, our initial mineral selection is composed mostly from the common primary and alteration mineral phases.

At the beginning of our experimentation, we have focused primarily on improving the system performance by uncovering a number of limitations and executing quick solutions to these problems. As a result, we have achieved an excellent stability of the interaction conditions, monitored by the pressure and temperature consistency throughout the experiments, and sufficient sampling precision and

ion analysis accuracy. Experiment-to-experiment repeatability of the final concentration response is the ultimate measure of both precision and accuracy, covering the whole process from sample preparation to data processing, and currently is within a relatively narrow error margin of 20% in most cases, as exampled in Figure 5.

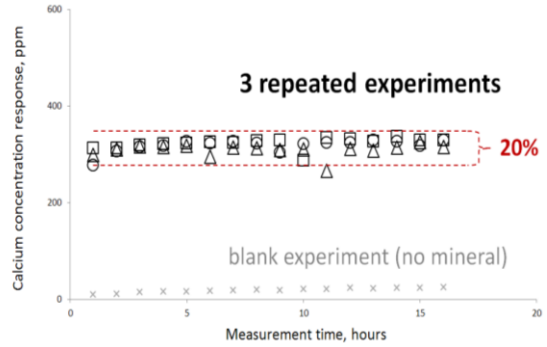

Figure 5 – Experiment-to-experiment repeatability.

Calcite equilibrated in CO_2-saturated water at 150 ^oC and 8.3 MPa pressure.

Our rock-fluid interaction system represents a high-throughput experimental setup that allows us to screen rapidly for changes in mineral solubility as a result of changing conditions or fluid environment. We can perform experiments using the whole water-CO_2 compositional spectrum. Figure 6 shows an example of resulting data streams from such an experiment, with a single mineral sample reaching equilibrium solubility in water over time in one reactor vessel, while in the other vessels is interacting with water-CO_2 mixtures of different compositions.

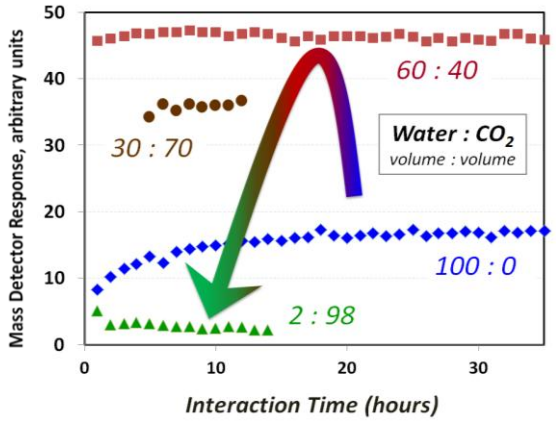

Figure 6 – Screening for mineral solubility changes across a wide range of fluid compositions.

Mineral sample: Barite; Particle sizes: 25-150 μm; Temperature: 100 ^oC; Pressure: 8.3 MPa.

Barite was chosen as an example simply because of its response fitting well within the range of a single plot, despite its disputable importance in geothermal applications (usually not naturally present, but introduced during drilling and causing some specific problems). It is apparent that its low initial aqueous solubility rapidly increases with increased amounts of dissolved CO_2, and then slowly decreases in solubility when separate fluid phases are created until becoming negligible in fairly dry supercritical CO_2 phase. This behavior is in agreement with what is known about barite in literature (Blount, 1977), and quite typical for many other minerals studied, but the magnitude of the response differs significantly. For example, calcite responds very promptly even to traces of CO_2 present, which makes it difficult to quantify as even perfectly deionized water absorbs some CO_2 immediately upon exposure to air. The importance of such a CO_2-responsiveness test is in the rapid determination of potential risk factors associated with large differences in rock and mineral solubilities across the whole range of water-CO_2 compositions, which may result in sealing-off a geothermal reservoir at the interface of those two fluids.

As opposed to screening a single mineral in whole range of fluid environments and/or under different conditions, we can also devote each vessel to individual minerals and screen such a mineral diversity against a fixed set of conditions. In the case when solubility is expected to change very little when going from one set of conditions to another, we can speed up the screening process by reusing the mineral sample already exposed to the previous set of conditions with a step change in conditions after reaching equilibrium solubility at the previous set of conditions. Figure 7 shows an example of such an experiment with diverse minerals in individual vessels and two sets of conditions applied in steps, one at the time. It appears that the increase in pressure results in somewhat lower solubilities of calcite and dolomite, higher solubility of anorthite, while quartz appears to be insensitive to pressure change. A slight increase of the background as measured for the blank fluid environment with no mineral present suggests that the observed changes might be within experimental error.

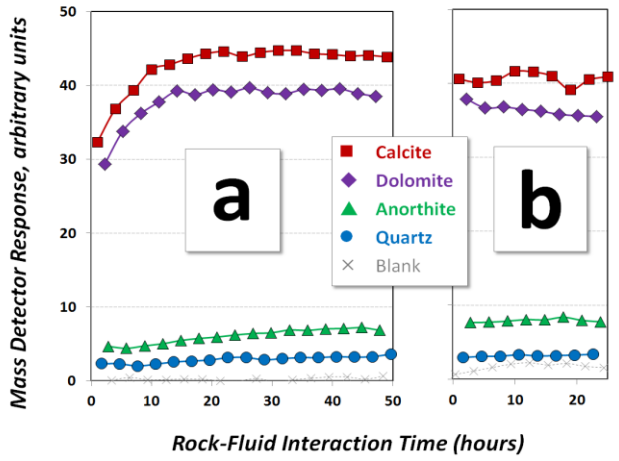

Figure 7 – Screening for diverse mineral solubilities at step-changed conditions.

Mineral samples: Calcite, Dolomite, Anorthite, Quartz, and no mineral (Blank); Particle sizes: 63-150 microns; Temperature: 120 ^{o}C; Pressure: 8.3 MPa (a) changed to 10.4 MPa (b).

The data on individual ion concentrations at different mineral-fluid interaction times represent the dissolution profile of each mineral at the specific set of experimental conditions, and can be combined into the overall mineral solubilities, or correlated with other parameters, including those important for modeling processes at a specific geothermal site. The information is still evolving, as we are repeating some of the most interesting experiments, taking into account additional experimental parameters such as the reactor channel and history of its use, and continuously improving our calibrations, curve fitting, and other data processing protocols.

While screening a broad combinatorial space of mineral solubilities, we proceed from known to unknown combinations of minerals, fluid environments, pressures, temperatures, and other conditions. The table in Figure 8 shows a summary of selected data obtained and processed for the presented study.

Rock Sample				Fluid Environment		Reactor Conditions		Ion Analysis Results				
Sample Name	Mineral Composition	Particle Size Min (µm)	Particle Size Max (µm)	Water (vol.%)	CO2 (vol.%)	Temperature (oC)	Pressure (psi)	Ion Detected	Concentration at 20 hrs (mg/L)	Concentration at 40 hrs (mg/L)	Concentration at 60 hrs (mg/L)	Concentration at 80 hrs (mg/L)
Calcite	Ca(CO)3	63	150	100	0	150	1200	Ca2+		12	17	
	Ca(CO)3	63	150	67	33	150	1200	Ca2+			164	173
	Ca(CO)3	63	150	56	44	150	1200	Ca2+	155	175	186	194
	Ca(CO)3	63	150	56	44	120	1200	Ca2+	245	283	306	322
Dolomite	MgCa(CO3)2	63	150	100	0	150	1200	Mg2+		3	4	
	MgCa(CO3)2	63	150	33	67	150	1200	Mg2+	54			
	MgCa(CO3)2	63	150	67	33	150	1200	Mg2+			50	53
	MgCa(CO3)2	63	150	56	44	120	1200	Mg2+	76	86	92	
	MgCa(CO3)2	63	150	100	0	150	1200	Ca2+		6	10	
	MgCa(CO3)2	63	150	33	67	150	1200	Ca2+	111			
	MgCa(CO3)2	63	150	67	33	150	1200	Ca2+			93	99
	MgCa(CO3)2	63	150	56	44	120	1200	Ca2+	151	171	182	
Anorthite	CaAl2Si2O8	63	150	100	0	150	1200	Ca2+		4	5	
	CaAl2Si2O8	63	150	33	67	150	1200	Ca2+	34			
	CaAl2Si2O8	63	150	67	33	150	1200	Ca2+			38	41
	CaAl2Si2O8	63	150	56	44	120	1200	Ca2+	21	24	26	
Microline	KAlSi3O8	25	63	100	0	120	1200	K+	8	9	10	10
	KAlSi3O8	25	63	100	0	150	1200	K+	5	6	6	7
	KAlSi3O8	25	63	56	44	150	1200	K+	9	10	11	12
	KAlSi3O8	25	63	56	44	120	1200	K+	7	8	9	10
Siderite	FeCO3	25	63	100	0	120	1200	Fe2+	12	13	15	15
	FeCO3	25	63	100	0	150	1200	Fe2+	10	11	12	12
	FeCO3	25	63	56	44	150	1200	Fe2+	44	52	56	59
	FeCO3	25	63	56	44	120	1200	Fe2+	48	54	58	61
Biotite	K(Mg,Fe)3AlSi3O10(F,OH)2	25	63	100	0	120	1200	K+	7	8	9	9
	K(Mg,Fe)3AlSi3O10(F,OH)2	25	63	100	0	150	1200	K+	9	10	10	11
	K(Mg,Fe)3AlSi3O10(F,OH)2	25	63	56	44	150	1200	K+	23	26	28	30
	K(Mg,Fe)3AlSi3O10(F,OH)2	25	63	56	44	120	1200	K+	24	28	30	31
	K(Mg,Fe)3AlSi3O10(F,OH)2	25	63	100	0	120	1200	Fe2+	14	16	18	19
	K(Mg,Fe)3AlSi3O10(F,OH)2	25	63	100	0	150	1200	Fe2+	14	16	17	18
	K(Mg,Fe)3AlSi3O10(F,OH)2	25	63	56	44	150	1200	Fe2+	59	67	72	76
	K(Mg,Fe)3AlSi3O10(F,OH)2	25	63	56	44	120	1200	Fe2+	66	75	80	84
	K(Mg,Fe)3AlSi3O10(F,OH)2	25	63	100	0	120	1200	Mg2+	22	26	28	30
	K(Mg,Fe)3AlSi3O10(F,OH)2	25	63	100	0	150	1200	Mg2+	18	20	22	23
	K(Mg,Fe)3AlSi3O10(F,OH)2	25	63	56	44	150	1200	Mg2+	34	38	41	43
	K(Mg,Fe)3AlSi3O10(F,OH)2	25	63	56	44	120	1200	Mg2+	34	39	42	44

Figure 8 – Ion solubilities for diverse minerals as measured by the PARC rock-fluid interaction system.

Diverse minerals, variety of fluid environments, and specific conditions selected as discussed in the paper.

Within the known space of mineral solubilities, we can compare our data with the behavior of the evaluated minerals as modeled previously based on published information. A wide variety of literature data is available, but it is often obtained at very different conditions, not interacted long enough, or obtained by using mineral samples containing unknown but likely different impurities. To get both representative and comparable data, LBNL has retrieved from their database the values that are based on all existing literature data and their calculations, assuming absolutely pure minerals and fluid environments.

Figure 9 compares the measured and modeled data for three different minerals. The absolute values show some discrepancies between measurements and modeling, most likely due to impurities present in both fluids (residual CO_2 acidity in water) and minerals (trace components with significant effect on dissolution of others) in our measurements, as well as a result of possible inaccuracies that might have been translated from literature values into the modeling data.

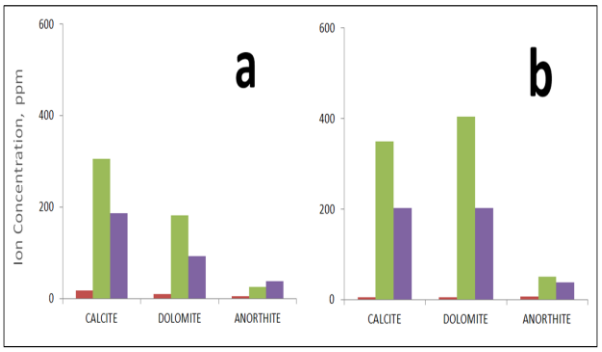

Figure 4 – Trends in the Ca^{2+} solubilities for calcite, dolomite, and anorthite.

As measured at PARC (a), versus modeled by LBNL using literature sources (b), in deionized water at 150 ^oC under 8.3 MPa (red), water saturated by CO_2 at 120 ^oC under 8.3 MPa (green), and water saturated by CO_2 at 150 ^oC under 8.3 MPa (purple).

Taking calcite as an example, we have observed that the values obtained by regular operation of our batch system are usually somewhat higher than those obtained in absolutely pure water previously (Segnit et al., 1962), primarily because of absorbing some CO_2 from our lab air with higher than usual CO_2 concentration and open contact with our water source (minimized in a special operation under helium). Also, even trace impurities present in the reacted mineral sample may influence or overshadow the actual concentration of the component of interest.

These phenomena are not surprising, as similar discrepancies between different experimental results are common and observed by others (for example, Morrow et al., 2001). The correlation between newly measured and previously published mineral solubility experimental data can be further improved by including additional parameters that affect the solubilities, if known, such as mineral impurities, fluid mixture pH or the CO_2 concentration in the local atmosphere. Nevertheless, the overall solubility trends are the same, confirming the sensitivity of calcite to the presence of CO_2 as well as lower solubility at higher temperatures.

SUMMARY AND CONCLUSIONS

PARC's multichannel Rock-Fluid Interactions System is fully operational, capable to simulate various underground conditions relevant to geothermal processes, and producing mineral solubility and dissolution data that can provide valuable knowledge on the behavior of well-known or unusual minerals in yet untested environments and/or under conditions not previously explored in the laboratory. While continuing to generate more batch solubility data, including going to untested territories, we are expecting to upgrade the system by installing a flow-through capability with a water-CO_2 circulation through a column packed by several rock samples, which may allow us to see effect of one dissolved mineral on dissolution/precipitation of others, among many other effects relevant to the CO_2-EGS reservoir development and operation.

The data will support a new modeling activity using the existing TOUGHREACT modules, and allow LBNL to enhance their models and improve the accuracy of the calculations, in order to capture the complexity of the situations with natural presence of CO_2 or other acidic gasses in existing hydrothermal reservoirs, as well as map out the process of the geochemical transition from aqueous to supercritical CO2-EGS.

ACKNOWLEDGEMENT

This work was supported by the U.S. Department of Energy, Geothermal Technologies Program, Energy Efficiency and Renewable Energy Office, Award No. DE-EE0002765.

We also thank the UC Berkeley Earth and Planetary Sciences Department for facilitating the rock sample characterization.

REFERENCES

André, L., Azaroual, M. and Menjoz, A. (2010), "Numerical Simulations of the Thermal Impact of Supercritical CO_2 Injection on Chemical Reactivity in a Carbonate Saline Reservoir," *Transp. Porous Med.*, **82**, 247-274.

Blount C.W. (1977), "Barite Solubilities and Thermodynamic Quantities up to 300 ^oC and 1400 bars," *Amer. Mineralogist*, **62**, 942-957.

Brown, D. (2000), "A Hot Dry Rock Geothermal Energy Concept Utilizing Supercritical CO_2 Instead of Water," *25th Workshop on Geothermal Reservoir Engineering, Stanford University*, 233–238.

Fouillac, C., Sanjuan, B., Gentier, S. and Czernichowski-Lauriol, I. (2004), "Could Sequestration of CO2 be Combined with the Development of Enhanced Geothermal Systems?," *3rd Annual Conference on Carbon Capture and Sequestration*, Alexandria, VA.

Garcia, J. (2001), "Density of Aqueous Solution of CO_2." *Lawrence Berkeley National Laboratory Report*, LBNL-49023, Berkeley, CA.

Kneafsey, T. and Pruess, K. (2010), "Laboratory Flow Experiments for Visualizing Carbon-Dioxide-Induced, Density-Driven Brine Convection," *Transp. Porous Med*, **82**, 123-139.

Liu, L., Suto, Y., Bignall, G., Yamasaki, N. and Hashida, T. (2003), "CO_2 injection to granite and sandstone in experimental rock/hot water systems", *Energy Conversion & Management*, **44**, 1399-1410.

McGrail, B.P., Schaef, H.T., Glezakou, V.A., Dang, L.X. and Owen, A.T. (2009), "Water Reactivity in the Liquid and Supercritical CO_2 Phase: Has Half the Story Been Neglected?," *Energy Procedia*, **1**, 3415–3419.

Morrow, C.A., Moore, D.E. and Lockner, D.A. (2001), "Permeability Reduction in Granite under Hydrothermal Conditions," *J. Geophys. Res.*, **106**, 30551-30560.

Palguta, J., Williams C.F., Ingebritsen, S.E., Hickman, S.H. and Sonnenthal, E. (2011), "An Approach to Modeling Coupled Thermal-Hydraulic-Chemical Processes in Geothermal Systems," *36th Workshop on Geothermal Reservoir Engineering, Stanford University*, 443-456.

Plaksina, T., White, C., Nunn, J. and Gray, T. (2011), "Effects of Coupled Convection and CO_2 Injection in Stimulation of Geopressured Geothermal Reservoirs," *36th Workshop on Geothermal Reservoir Engineering, Stanford University*, 146-154.

Pruess, K. (2006), "Enhanced geothermal systems (EGS) using CO2 as working fluid – a novel approach for generating renewable energy with simultaneous sequestration of carbon," *Geothermics*, **35**, 351-367.

Pruess, K. and Azaroual, M. (2006), "On the Feasibility of using Supercritical CO_2 as Heat Transmission Fluid in an Engineered Hot Dry Rock Geothermal System," *31st Workshop on Geothermal Reservoir Engineering, Stanford University*, 386–393.

Pruess, K. (2008), "On Production Behavior of Enhanced Geothermal Systems with CO_2 as Working Fluid," *Energy Conversion and Management*, **49**, 1446–1454.

Regnault, O., Lagneau, V., Catalette, H., Schneider, H. (2005), "Étude Expérimentale de la Réactivité du CO_2 Supercritique vis-à-vis de Phases Minérales pures, Implications pour laSequestration Géologique de CO_2.," *C. R. Geoscience*, **337**, 1331–1339.

Rosenbauer, R.J., Koksalan, T. and Palandri, J.L. (2005), "Experimental investigation of CO_2-brine-rock interactions at elevated temperatures and pressure: Implications for CO_2 sequestration in deep-saline aquifers," *Fuel Proc. Tech.*, **86**, 1581-1597.

Salimi, H., Groenenberg, R. and Wolf, K.-H. (2011), "Compositional Flow Simulations of Mixed CO_2-Water Injection into Geothermal Reservoirs: Geothermal Energy Combined With CO_2 Storage," *36th Workshop on Geothermal Reservoir Engineering, Stanford University*, 169-181.

Segnit E.R., Hollanda H.D. and Biscardi C.J., (1962), "The Solubility of Calcite in Aqueous Solutions – I. The Solubility of Calcite in Water between 75° and 200° at CO_2 Pressures up to 60 atm," *Geochim. Cosmochim. Acta*, **26**, 1301-1331.

Steefel, C.I., DePaolo, D.J. and Lichtner, P.C. (2005), "Reactive Transport Modeling: An Essential Tool and a New Research Approach for the Earth Sciences," *Earth Planet. Sci. Lett.*, **240**, 539–558.

Tester, J.W., Anderson, B., Batchelor, A., Blackwell, D., DiPippo, R., Drake, E., Garnish, J., Livesay, B., Moore, M.C., Nichols, K., Petty, S., Toksoz, N., Veatch, R., Augustine, C., Baria, R., Murphy, E., Negraru, P. and Richards, M., (2006), "The future of geothermal energy: Impact of enhanced geothermal systems (EGS) on the United States in the 21st century," *Massachusetts Inst. Technology, Final Report for the DOE Contract DE-AC07-05ID14517*.

Ueda, A., Kato, K., Ohsumi, T., Yajima, T., Ito, H., Kaieda, H., Meycalf, R. and Takase, H. (2005), Experimental Studies of CO_2-Rock Interaction at Elevated Temperatures under Hydrothermal Conditions," *Geochem. J.*, **39**, 417–425.

Wan, Y., Xu, T. and Pruess, K. (2011), "Impact Of Fluid-Rock Interactions on Enhanced Geothermal Systems with CO_2 as Heat Transmission Fluid," *36th Workshop on Geothermal Reservoir Engineering, Stanford University*, 792-801.

Xu, T., Apps, J.A. and Pruess, K. (2004), "Numerical Simulation of CO_2 Disposal by Mineral Trapping in Deep Aquifers," *Appl. Geochem*., **19**, 917–936.

Xu, T., Sonnenthal, E.L., Spycher, N., and Pruess, K. (2006), "TOUGHREACT: A Simulation Program for Non-isothermal Multiphase Reactive Geochemical Transport in Variably Saturated Geologic Media," Computers & Geosciences, 32, 145-165.